

# Influence of the voltage pulse front shortening on the pulse repetition rate in a copper vapour laser

P.A. Bokhan, P.P. Gugin, D.E. Zakrevskii, M.A. Lavrukhin, M.A. Kazaryan, N.A. Lyabin

**Abstract.** The lasing characteristics of a copper vapour laser are investigated in the regime of a pulse train excited in the internal-heating tube with the diameter of 2 cm and length of 48 cm. Two power supply schemes are compared: a conventional scheme with a storage capacitor discharged through a thyatron connected to a peaking capacitor and the scheme in which the peaking capacitor is connected to the laser active element through a kivotron – a fast switch based on the ‘open discharge’ with a turn-on time of less than 1 ns. It is shown that in the considered range of the pulse repetition rates  $f = 2–16$  kHz in the first case we deal with a typical energy dependence on frequency having a maximum near 4–5 kHz. In the second case, the lasing energy is frequency-independent; hence, the average power in this range is proportional to  $f$ . The results obtained are explained by the neutralised influence of the initial electron concentration on energy characteristics of the copper vapour laser.

**Keywords:** copper vapour laser, gas discharge, current switch, lasing energy.

## 1. Introduction

Copper vapour lasers (CVLs) with the emission wavelengths  $\lambda_1 = 511$  nm and  $\lambda_2 = 578$  nm have dominated for a long time over other pulsed lasers of the visible range in such combined parameters as the average output power, repetition rate of nanosecond pulse lasing, efficiency and so on. In the last decade they have been in many fields replaced by the solid-state diode-pumped lasers with intracavity wavelength conversion to the visible range. However, one may assert that the possibilities of CVLs are not exhausted because there are, at least, three global unsolved problems concerning the lasers on self-terminated transitions, including CVLs, which prevent attaining the limiting and sufficiently high parameters inherent in the nature of these types of lasers [1, 2]:

1. Low actual efficiency of 1%–2% [3], which is at the level of first achievements [1, 4] and by an order of magnitude less than the value theoretically predicted from the rates of

elementary processes for an ideal (rectangular) excitation pulse [5, 6].

2. Low pulse repetition rate (PRR) of lasing at the maximal or close to it lasing efficiency, which is two orders lower than the PRR determined by the rate of deactivation of metastable states [7, 8].

3. Lack of switches satisfying the requirements to the pump systems of repetitively pulsed lasers on self-terminated transitions.

In the present work we present first results on investigating the influence of shortening the leading edge duration of the voltage pulse to  $\sim 1$  ns on the energy-frequency characteristics of CVLs. In the framework of the problems formulated above the investigation is aimed at solving the third problem, namely, the development of an ideal switch for the CVL power supply system.

## 2. Experimental

For solving the problem stated we developed an ‘open discharge’ switch – kivotron [9]; its principle of operation and switching characteristics are discussed in [10]. In contrast to coaxial constructions [9, 10], in the present work we employed the planar geometry of a ‘sandwich’ kivotron shown in Fig. 1. The kivotron comprises two identical accelerating (discharge) gaps 3 mm in length each, separated by the drift space with a total length of 14 mm. The discharge gaps are formed by the titanium cathodes having polished working parts with a diameter of 4 cm and metal grids from molybdenum with the geometrical transparency of  $\sim 92.5\%$ . Both the grids have a galvanic contact and form the first low-inductance input, which is usually grounded through a current shunt. The cathodes are also connected with each other and form the second low-inductance high-voltage input. The self-capacity for each discharge gap is  $\sim 50$  pF; it is the main factor that limits above the rate of kivotron switching. The current–voltage dependences  $I(U_0)$  of the kivotron in the regime of electron beam generation are presented in Fig. 2 ( $U_0$  is the initial voltage across the capacitor) along with dependences of duration of current pulse through the kivotron  $\tau_I(U_0)$  at the working capacitance of 0.85 nF and helium pressures  $p_{\text{He}} = 20$  and 5 Torr, respectively (with the current shunt of 0.64  $\Omega$ ). In the same figure, the switching characteristic of the kivotron  $\tau_{\text{sw}}(U_0)$  is shown ( $\tau_{\text{sw}}$  is the time of switching) in helium at  $p_{\text{He}} \approx 14$  Torr and an active load of 25  $\Omega$ . One can see that the time of kivotron transit to a low-resistance state, which is equal to the discharge time of the self-capacity  $C_k \sim 100$  pF, is less than 1 ns at the opening voltage  $U_0 > 10$  kV. The residual voltage across the kivotron usually does not exceed

P.A. Bokhan, P.P. Gugin, D.E. Zakrevskii, M.A. Lavrukhin A.V.

Rzhanov Institute of Semiconductor Physics, Siberian Branch, Russian Academy of Science, prosp. Akad. Lavrent'eva 13, 630090 Novosibirsk, Russia; e-mail: zakrdm@isp.nsc.ru;

M.A. Kazaryan P.N. Lebedev Physics Institute, Russian Academy of Sciences, Leninsky prosp. 53, 119991 Moscow, Russia;

N.A. Lyabin Research and Production Corporation ‘Istok’, ul. Vokzalnaya 2a, 141190 Fryazino, Moscow region, Russia

Received 7 November 2012; revision received 6 February 2013

*Kvantovaya Elektronika* 43 (8) 715–719 (2013)

Translated by N.A. Raspopov

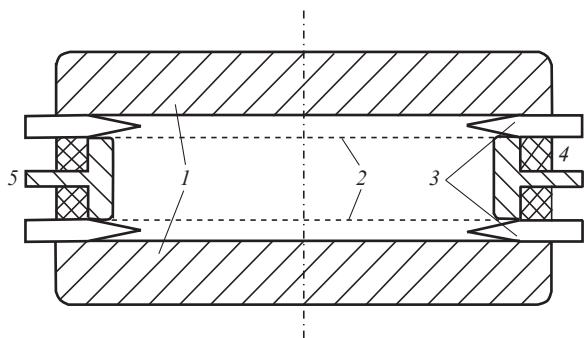


**Figure 1.** Schematic diagram of the kivotron: (1) cathode; (2) grid anode; (3, 4) dielectric separating rings; (5) current lead.

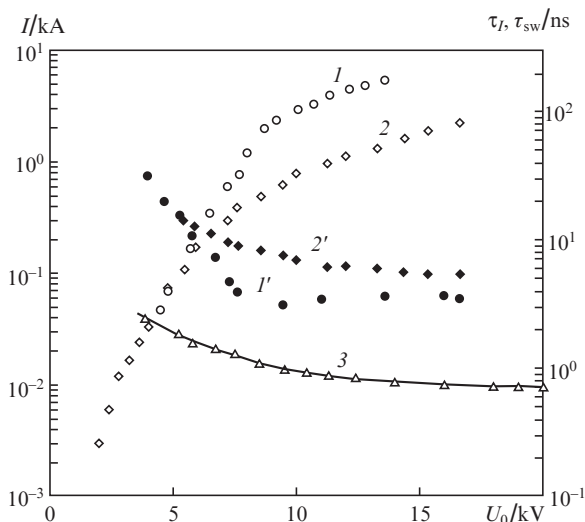


**Figure 2.** Volt-ampere characteristics of the kivotron (1, 2) and duration of current pulse through the kivotron (1', 2') in the regime of electron beam generation; the switching characteristic (3) at  $p_{\text{He}} = (1, 1')$  20, (2, 2') 5 and (3) 14 Torr.

$\sim 1-1.5$  kV, which corresponds to the switching efficiency of more than 90% at  $U_0 \sim 20$  kV.

In the experiments we used a gas-discharge tube (GDT) with the length  $l = 48$  cm and diameter of the discharge channel  $d = 2$  cm, produced by the Research and Production Corporation 'Istok' by the technology described in [3]. A

technical improvement of the GDT is the heating coil made of the W-Re alloy [11]. The coil wound directly on the internal alumina discharge tube was connected to the GDT electrodes. Specific constructive features of the GDT provided its operation at temperatures up to  $T = 1420^\circ\text{C}$  (the temperature was measured by a pyrometer). At a higher temperature, a spontaneous ignition of the arc discharge may occur if the voltage across the heating coil exceeds 100 V. The coil is simultaneously the working inductance, which shunts the discharge gap ( $L_{\text{sh}} \approx 40 \mu\text{H}$ ). The self-inductance of the GDT with a coaxial backward conductor  $L_1$  is  $\sim 1.6 \times 10^{-7}$  H.

Schematic diagrams of the GDT power supply are presented in Fig. 3. In the first case (Fig. 3a) the power supply has an ordinary scheme in which the storage capacitor  $C_0$  discharges through a thyatron to the peaking (working) capacitor  $C_p$  connected directly to the GDT electrodes. Use was made of the optimal capacitance  $C_0 \approx 15d^2/l \approx 1.5$  nF [12] and two capacitors  $C_p$ :  $C_p = C_0$  and  $C_p = 0.5C_0$ . In the second case (Fig. 3b), the peaking capacitor  $C_p = C_0$  discharges through the GDT that is connected in series with the kivotron. In order to prevent a potential difference between the GDT electrodes in the course of the capacitor  $C_p$  charging, a voltage was applied to the kivotron cathode connected with the GDT anode through the circuit  $L_k - C_k$  with the condition  $C_k L_k = C_p L_p$  fulfilled ( $L_p$  is the recharge circuit inductance). The charge time for the corresponding capacitors  $\tau = \pi(L_i C_i)^{1/2} \sim 100$  ns was taken equal to the lag of the discharge through the kivotron. The scheme for measuring the electrical parameters (voltage and current) was similar to that in [10].

In all cases the storage capacitor  $C_0$  was charged from a pulse step-up transformer triggered by a transistor switch. The optimal working voltage across  $C_0$  corresponding to a maximal efficiency was 12–14 kV and the pulse repetition rate was below 16 kHz. Measurements of frequency-energy characteristics at a constant energy of the pump pulses (or at constant voltage across the capacitor  $C_0$ ) are hindered by a considerable variation of the temperature regime of the GDT and, consequently, non-stationary conditions of laser generation. Hence, all the measurements were performed in the regime of the pulse train applied at the instant of changing the polarity of the alternating voltage feeding the heating coil [11]. Usually the pulse train duration was no longer than 2 ms. Under a longer duration, a low-voltage arc may occur between the electrodes of the GDT at every temperature of the latter. Because the heating coil was powered from the line voltage, the pulse train repetition rate was chosen 50 Hz and synchronised with the line voltage frequency.

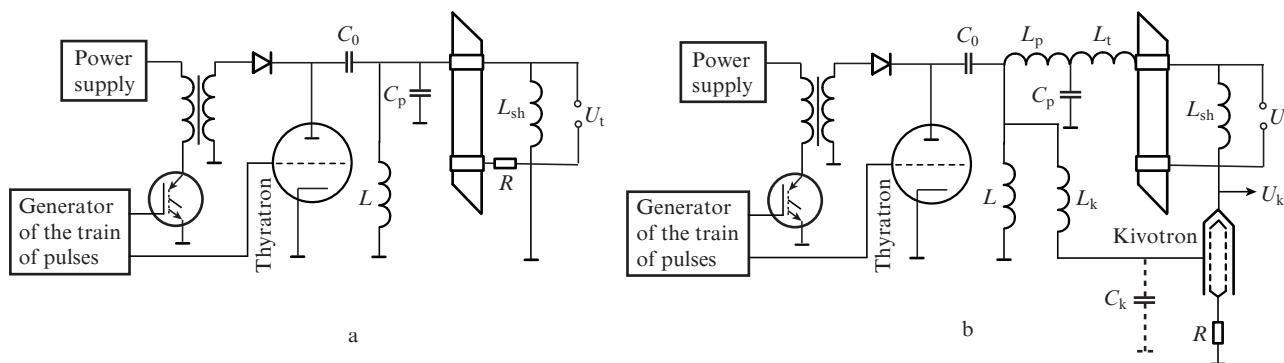


**Figure 3.** Power supply unit for the CVL active element: discharge of  $C_0$  through a thyatron (a) and discharge of  $C_p$  to GDT through a kivotron (b).

### 3. Results of studying the frequency – energy characteristics of the CVL

Figure 4 shows the evolution of laser generation under pumping by a pulse train. One can see that lasing is observed starting from the second exciting pulse and from the third pulse up to the train end the lasing energy has a constant value at optimal  $U_0$  (up to 14 kV). At a higher voltage ( $U_0 > 16$  kV), the lasing pulses have equal intensities starting from the second pulse. Such a behaviour is explained by the fact that due to the small initial electron concentration  $n_{e0}$  at the instant of the first pulse the breakdown develops sufficiently slowly so that the time evolution of the voltage across the tube is of oscillatory character (because of the small  $L_{sh}$ ) up to the instant of breakdown. After the breakdown, the oscillations cease; however, the residual voltage is too low to excite generation.

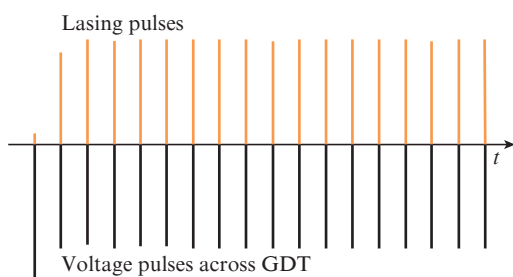


**Figure 4.** The typical evolution of laser generation powered by a train of pulses ( $U_0 < 14$  kV).

Oscillograms of the voltage pulses across the GDT ( $U_t$ ), current through the tube ( $I_t$ ) and lasing ( $P_p$ ) are presented in Fig. 5; the main characteristics of lasing at  $T = 1420^\circ\text{C}$  are shown in Fig. 6 (the pressure of neon is  $p_{Ne} \approx 40$  Torr). One can see a good matching of the power supply with the GDT at  $C_0 = C_p = 1.5$  nF (Figs 5a and 5b). It is revealed in that the peak of the lasing pulse coincides with the current peak and the amplitude of the reflected voltage pulse does not exceed 10% of the main pulse amplitude. Hence, despite the non-optimal GDT temperature ( $1420^\circ\text{C}$  as compared to  $1550$ – $1600^\circ\text{C}$  in [3]), the lasing efficiency  $\eta$  with respect to the energy stored in  $C_0$  amounts to 0.66%.

At  $C_p = 0.5C_0$ , the matching is noticeably worse (Fig. 5c). The worse matching quality results in a reduced average ( $P_{av}$ ) and pulse ( $P_p$ ) lasing power as compared to the case  $C_0 = C_p$  [curves (1) and (2) in Fig. 6]. Nevertheless, in the case  $C_0 = C_p$ , the extreme dependences of the energy  $W$  [curve (3)] and lasing efficiency  $\eta$  [curve (4)] on the PRR  $f$  are realised. Maximal values of these dependences are observed in the range of the PRR  $f = 3$ – $6$  kHz, where they are almost constant. At  $f < 3$  kHz, the reduction of  $W$  and  $\eta$  is explained by a considerable delay of the GDT discharge start due to a fall of  $n_{e0}$  at lower  $f$ . In the result, a fraction of energy transferred to capacity  $C_p$  is lost in the heating coil, which makes  $W$  and  $\eta$  lower. At  $f > 6$  kHz, a typical reduction of  $W$  and  $\eta$  with increasing  $f$  is observed, which is explained by the enhanced influence of  $n_{e0}$  on lasing characteristics. At  $f > 14$  kHz the average lasing power  $P_{av}$  falls as well.

Oscillograms of the initial parts of the pulse voltage  $U_t$  across the GDT, currents through kivotron  $I_k$  and through the GDT  $I_t$ , and the lasing intensity are shown in Fig. 7. One

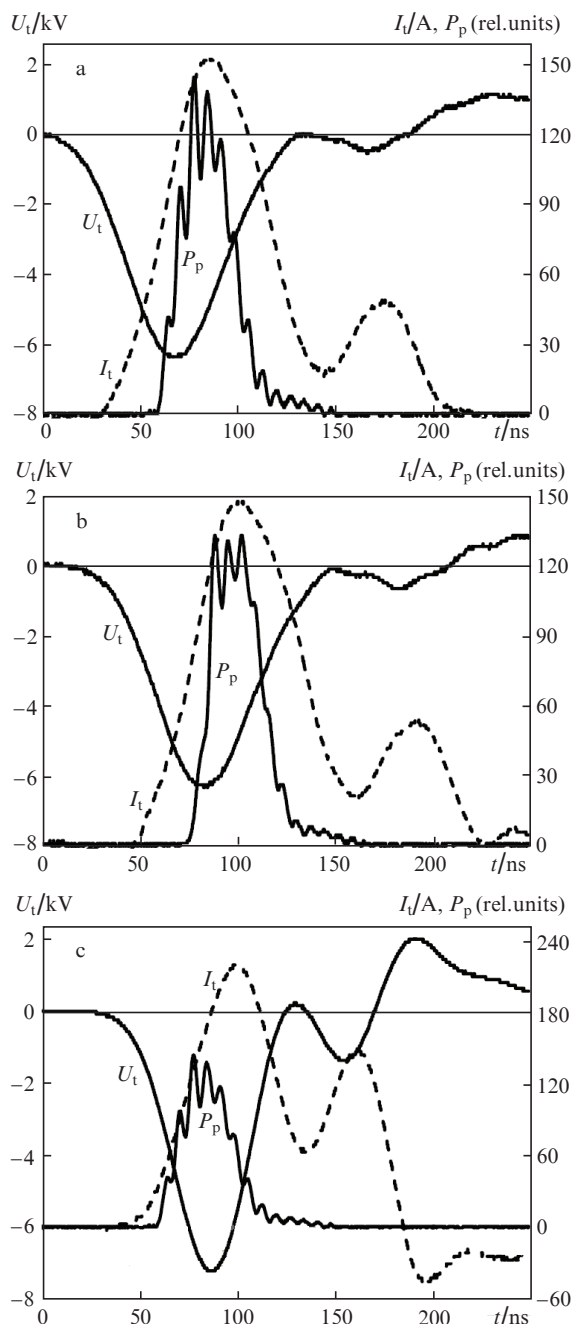


**Figure 5.** Oscillograms of voltage  $U_t$  and current  $I_t$  pulses and the second (a) and fifth (b, c) pulses from the generation train of pulses ( $P_p$ ) for the scheme in Fig. 3a at  $T = 1420^\circ\text{C}$ ,  $p_{Ne} \approx 40$  Torr,  $C_0 = C_p = 1.5$  nF (a, b) and  $C_0 = 2C_p = 1.5$  nF (c).

can see that the maximal voltage  $U_t$ , which is close to the charge voltage across  $C_0$ , is attained in  $\sim 1.5$  ns. The slight delay in the voltage pulse  $U_t$  as compared to the data from Fig. 2 is explained by self-capacitances and laser tube inductance. The start of the current oscillogram  $I_k$  does not correspond to the real current through the GDT, because the oscillogram expresses the discharge of the kivotron self-capacitance through the current shunt. The increase in the voltage  $U_t$  is observed later than that of kivotron current for the same reason. A real oscillogram of the current through the GDT  $I_t$  is obtained by subtracting from the current oscillogram  $I_k$  the oscillogram of kivotron ‘idle current’ recorded without capacity  $C_p$  under the condition  $C_k = C_0$

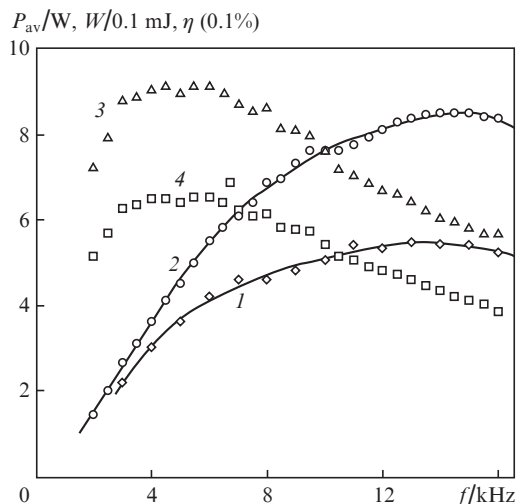


**Figure 6.** Lasing characteristics vs. PRR for the scheme shown in Fig. 3a: average power  $P_{av}$  (1, 2), pulse energy  $W$  (3), and efficiency  $\eta$  (4);  $C_0 = 2C_p$  (1) and  $C_0 = C_p$  (2–4).

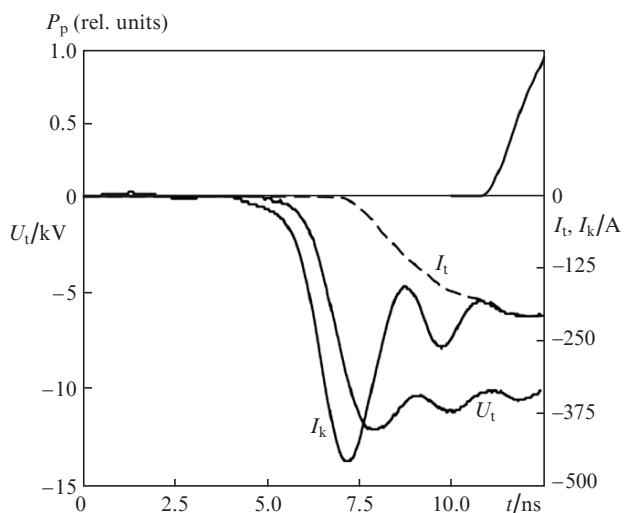


**Figure 7.** Oscillograms of the pulses of voltage  $U_t$ , current  $I_t$  and  $I_k$ , and lasing ( $P_p$ ) for the scheme shown in Fig. 3b.

and with lacking load (except for the current shunt) in the kivotron circuit.

The frequency–energy characteristic of the laser excited by the scheme comprising the kivotron is shown in Fig. 8. One can see that the output power increases almost linearly up to the frequency  $f = 16$  kHz [curve (1)] limited by the employed power supply [no PRR dependence of  $W$  is observed in curve (2)]. For comparison, the lasing characteristics for the optimised conventional exciting scheme are presented for  $C_0 = C_p$  [curves (3, 4)].

#### 4. Discussion of results

The data obtained in the present work confirm the results of many previous reports on a crucial influence of the pre-pulse electron concentration  $n_{e0}$  on the limitation of frequency–energy characteristics of the CVL, which were generalised in [13, 14]. Presently, the influence of  $n_{e0}$  is most

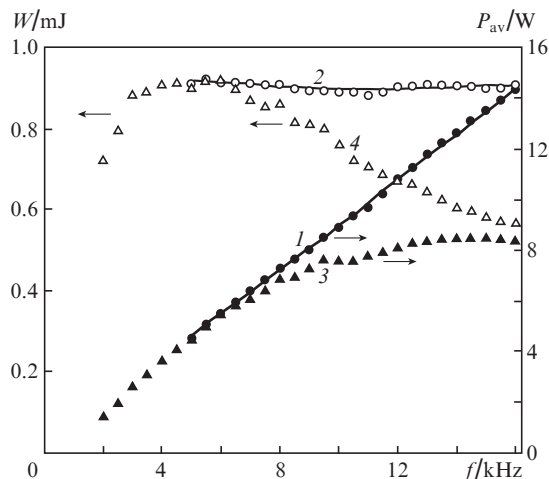


**Figure 8.** Lasing characteristics vs. PRR with the employment of the kivotron in the power exciting scheme (Fig. 3b) (1, 2) and with conventional exciting scheme (Fig. 3a) (3, 4). In both the cases  $C_0 = C_p$ .

successfully neutralised in hybrid lasers, in which the lasing efficiency  $\eta \approx 3.8\%$  [15] and average linear lasing power of  $155 \text{ W m}^{-1}$  [14] were obtained (the GDT with the diameter  $d = 3.8$  cm in the amplification regime).

It was shown [13] that by neutralising the influence of  $n_{e0}$  in the ‘Kristall LT-40 Cu’ active elements produced by the Research and Production Corporation ‘Istok’ (the GDT with the diameter  $d = 2$  cm, length  $l = 125$  cm) [3] it is possible to realise a linear growth of the lasing linear power actually up to  $200 \text{ W m}^{-1}$ . We may compare the results of the present work (Fig. 8) with those from [13] (Fig. 9). One can see an almost identical behaviour of  $P_{av}$  versus  $f$  (up to 16 kHz) in using for switching both a thyatron (the present work) and a vacuum tube [13]; see curve (3) in Fig. 8 and curve (1) in Fig. 9, respectively. The vacuum tube and thyatron pumping were compared in [3] with actually similar results obtained. If a kivotron is used for switching then the linear character of output power dependence on  $f$  is observed up to at least  $f = 16$  kHz, which is similar to the theoretical dependence (2) in Fig.

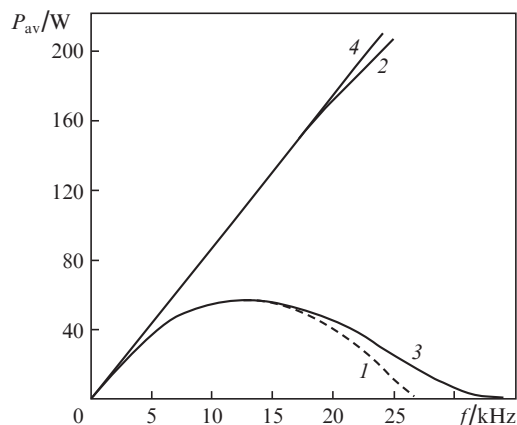


**Figure 9.** Lasing characteristics vs. PRR obtained in [13]: calculated output power  $P_{av}$  vs. PRR  $f$  with the allowance made for  $N_{e0}$  and  $n_{ms0}$  (1),  $n_{ms0}$  only (2), and  $n_{e0}$  only (3), and a linear dependence of  $P_{av}$  (4).

9 obtained with only the pre-pulse concentration of metastable states  $n_{ms0}$  taken into account.

Based on these results one may conclude that employing the switching device with the turn-on time of  $\sim 1$  ns (Fig. 2) it is possible to neutralise the influence of  $n_{e0}$  related with the parasitic population of metastable copper states in the leading edge of the pump pulse at the PRR of at least 16 kHz. Note that the linear average pump power of the pulse train in this case is  $\sim 5$  kW m<sup>-1</sup> at  $U_0 = 14$  kV. Hence, one may assume that under the optimised temperature operation of the GDT, the average output power in the train will be noticeably higher than that obtained in the present work ( $\sim 14.5$  W or  $\sim 30$  W m<sup>-1</sup>, Fig. 8) even at  $f = 16$  kHz. One may also assume that at higher  $f$  the average lasing power will increase faster than  $f$ , because a progressively less fraction of the pump pulse energy would be spent on plasma production. Such a tendency is just seen in Fig. 8 [curve (2)].

## 5. Conclusions

The study conducted shows that employment of the kivotron – a switching device based on an ‘open discharge’ with the turn-on time of  $\sim 1$  ns makes it possible to neutralise the influence of the pre-pulse electron concentration  $n_{e0}$  on frequency–energy characteristics of the CVL at the pulse repetition rate of at least 16 kHz in the GDT with the discharge channel diameter of 2 cm. Hence, the switching device used in the present work may be considered as an ideal ‘switch’ for copper vapour laser supplying systems.

**Acknowledgements.** The work was supported by State Contracts (Nos 11.519.11.6037 and 14.518.11.7008).

## References

1. Walter W.T., Solimene N., Piltch M., Gould G. *IEEE J. Quantum Electron.*, **2**, 474 (1966).
2. Petrash G.G. *Usp. Fiz. Nauk*, **105**, 645 (1971) [*Sov. Phys. Usp.*, **14**, 747 (1972)].
3. Grigor'yants A.G., Kazaryan M.A., Lyabin N.A. *Lazery na parakh medi* (Copper Vapour Lasers) (Moscow: Fizmatlit, 2005).
4. Isaev A.A., Kazaryan M.A., Petrash G.G. *Pis'ma Zh. Eksp. Teor. Fiz.*, **16**, 40 (1972).
5. Batenin V.M., Vokhmin P.A., Klimovskii I.I., Selezneva L.A. *Teplofiz. Vys. Temp.*, **20**, 177 (1982).
6. Batenin V.M., Boichenko A.M., Buchanov V.V., Kazaryan M.A., Klimovskii I.I., Molodykh E.I. *Lazery na samoogranichennykh perekhodakh atomov metallov* (Lasers on Self-Contained Transitions of Metal Atoms) (Moscow: Fizmatlit, 2009) Vol. 2.
7. Bokhan P.A. *Kvantovaya Elektron.*, **13**, 1837 (1986) [*Sov. J. Quantum Electron.*, **16**, 1207 (1986)].
8. Bokhan P.A., Zakrevskii D.E. *Zh. Tekh. Fiz.*, **67** (5), 54 (1997).
9. Bokhan P.A. Bulletin of Invention No. 1644686, priority date 16.01.1989.
10. Bokhan P.A., Gugin P.P., Zakrevskii D.E., Lavrukhin M.A. *Pis'ma Zh. Tekh. Fiz.*, **38** (8), 63 (2012).
11. Bokhan P.A., Gerasimov V.A. Bulletin of Invention No. 755136, priority date 09.01.1979; Bokhan P.A., Gerasimov V.A. Brevet d'invention No. 2529401. Date de depot 28.06.1982.
12. Bokhan P.A., Gerasimov V.A. *Kvantovaya Elektron.*, **6**, 451 (1979) [*Sov. J. Quantum Electron.*, **9**, 273 (1979)].
13. Bokhan P.A., Zakrevskii D.E. *Kvantovaya Elektron.*, **32**, 602 (2002) [*Quantum Electron.*, **32**, 602 (2002)].
14. Withford M.Y., Brown D.J.W., Mildren R.P., Carman R.J., Marshall G.D., Piper J.A. *Prog. Quantum Electron.*, **28**, 165 (2004).
15. Le Guadec E., Coutance P., Bertrand G., Peltier C.A. *IEEE J. Quantum Electron.*, **35**, 1616 (1999).